

HOMOGENIZATION OF TWIN-ROLL CAST Al-Li-BASED ALLOY STUDIED BY IN-SITU ELECTRON MICROSCOPY

¹Miroslav CIESLAR, ¹Barbora KŘIVSKÁ, ¹Rostislav KRÁLÍK, ¹Lucia BAJTOŠOVÁ,
²Olexandr GRYDIN, ²Mykhailo STOLBCHENKO, ²Mirko SCHAPER

¹Charles University, Faculty of Mathematics and Physics, Prague 2, Czech Republic, EU,
cieslar@met.mff.cuni.cz, krivska.barbora@seznam.cz, rkralik96@seznam.cz, lucibajtos@gmail.com

²Paderborn University, Chair of Materials Science, Paderborn, Germany, EU,
gyrdin@lwk.upb.de, stolbchenko@lwk.upb.de, schaper@lwk.upb.de

<https://doi.org/10.37904/metal.2022.4438>

Abstract

Transformation of Fe- and Cu-rich primary phase particles was studied in an Al-Li-based alloy prepared by twin-roll casting. Thin foils for combined STEM and SEM experiments were prepared by electrolytic twin-jet polishing. They were in-situ heated in a TEM heating stage and observed at 200 kV in the JEOL JEM 2200FS electron microscope equipped with STEM HAADF and BF detectors and SEM BSE and SE detectors working both in composition and topographic modes. The resulting structures were combined with EDS mapping performed directly in the heating holder. Dissolution and transformation of Cu- and Fe-rich particles occur above 500 °C. EDS maps acquired on the foil cooled down to room temperature show that Cu and Fe are both still present in newly formed particles, most likely indicating the presence of the Al₇Cu₂Fe phase.

Keywords: Al-Li-based alloy, in-situ TEM, homogenization, phase transformation

1. INTRODUCTION

New Al-Li-based alloys have been widely used in aerospace, aviation, and military applications thanks to their high strength, low density, good corrosion resistance, and fracture toughness [1-4]. The superior properties of Al-Li alloys follow from the addition of Li. Adding one wt% of Li decreases the density of the alloy almost by 3 % and increases the elastic modulus by 6 % [4, 5]. Li-containing aluminum alloys also have a higher resistance to fatigue crack-growth and stress-corrosion cracking than traditional ones [6, 7]. Other alloying elements, such as Cu and Mg, commonly added to high-strength Al-Li alloys, produce different strengthening phases contributing to the total strengthening of the material [5,8,9]. The third generation of Al-Li alloys contains mainly plate-like precipitates of the T₁ (Al₂CuLi) phase, plates of the θ' (Al₂Cu) phase, and rods of the S' (Al₂CuMg) phase [10,11]. Zr addition improves the stability of the microstructure imposed by an intensive plastic deformation of billets by forming a dispersion of the β' (Al₃Zr) phase precipitating during long-term homogenization of initial ingots at high temperatures [5]. Several attempts to improve the properties of Al-Li alloys by a microalloying with Sc were mentioned in the literature [12,13]. Fine precipitates of the Al₃Sc (or Al₃(Sc,Zr) in the case of Zr-containing alloys) could further improve the strength and structure stability of the material. Generally, they form during annealing in the temperature interval of 300-480 °C. However, long-term homogenization annealing of the material at high temperatures (above 500 °C), typical for direct-chill (DC) cast alloys, is necessary to dissolve coarser primary phases in highly alloyed Cu and Mg containing alloys. Exposure of Al₃(Sc,Zr) particles to such a high temperature is responsible for their significant growth and coarsening [14] and the advantageous strengthening effect loss. Finer primary phase particles and significantly more homogeneous distribution of solutes could be reached in Al materials cast at lower gauges (typical for twin-roll casting (TRC)) [15]. The use of lower temperatures and shorter annealing times necessary for their homogenization could be expected.

New Al-Li-Cu-Mg-Zr alloy microalloyed with Sc was prepared by TRC [16]. A refining role of Sc addition on the initial microstructure was confirmed. The present contribution is focused on studying the evolution of primary phase particles during high-temperature annealing. A treatment simulating homogenization of the as-cast structure was investigated using in-situ scanning electron microscopy and energy dispersive spectroscopy.

2. EXPERIMENTAL DETAILS

The preparation of the experimental TRC alloys is described in detail elsewhere [16]. The chemical composition of the experimental alloy is shown in **Table 1**.

Table 1 Chemical composition of Al-Li-Cu-Mg alloys (wt%)

Al	Cu	Li	Mg	Zr	Ag	Sc	Other
96.0	2.5	0.7	0.3	0.1	0.3	0.17	Balance

Thin foils for combined (scanning) transmission electron microscopy ((S)TEM) and scanning electron microscopy (SEM) experiments were prepared by electrolytic twin-jet polishing in a 30% nitric acid in methanol at -20 °C. They were in-situ step-by-step heated (step 50 K/30 min) in a TEM/STEM heating stage from 300 °C up to 550 °C and observed at 200 kV in the JEOL JEM 2200FS electron microscope equipped with STEM high angle annular dark field (HAADF) and bright field (BF) detectors, and SEM backscattered electron (BSE) and secondary electron (SE) detectors working both in composition and topographic modes. The resulting structures were combined with energy dispersive spectroscopy (EDS) mapping performed directly in the heating holder (tantalum furnace) using a silicon drift detector (SDD) that collects X-rays from (S)TEM samples at a large solid angle (0.98 steradians) from a detection area of 100 mm².

3. RESULTS AND DISCUSSION

Figure 1 shows STEM HAADF, and STEM BF images of a typical intermetallic particle in a thicker zone of the specimen (~300 nm estimated from a convergent beam in TEM) coupled with distribution maps of Fe, Cu, and Al in the as-cast material. More detailed local EDS chemical analyses were performed in selected points marked by crosses in **Figure 1a**. The concentrations measured in point 1 (60 at% Al, 6 at% Fe, 33 at% Cu, 1 at% Mg, Li could not be detected by EDS; all other elements could be neglected within the experimental error) most probably indicate the presence of the Al₇Cu₂Fe phase reported in technical high-strength aluminum alloys [17].

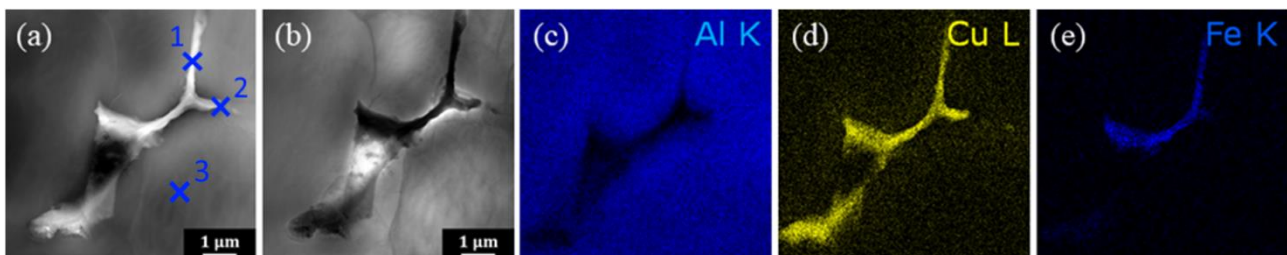


Figure 1 STEM HAADF (a), STEM BF (b), and distribution maps of Al (c), Cu (d), and Fe (e) in the primary phase particle

The local analysis in the Fe-free zone marked by the number 2 (52 at% Al, 47 at% Cu, 1 at% Mg, similarly, as in point 1, the concentration of Li could not be evidenced by EDS, and concentrations of other elements are negligible within the experimental error) suggests the presence of the AlCu phase. Generally, the Al₂Cu phase is reported in the initial states of Cu-containing Al alloys [17]. Nevertheless, the appearance of the AlCu phase could not be entirely excluded because its formation in highly non-equilibrium Al-based alloys is reported in the literature [18]. Alternatively, the detected high concentration of Cu might be an artifact given by absorption

of the Al EDS signal inside the particle. Small concentrations of Mg atoms detected by EDS in both positions most probably appear due to excitation of the surrounding Al matrix containing dissolved magnesium. However, partial segregation of Mg on grain boundaries could not be excluded. The lack of Sc or Zr inside the primary phase particles indicates that they are both dissolved inside the aluminum matrix. A local EDS analysis performed in the matrix (point 3 in **Figure 1a** - 96.9 at% Al, 2.2 at% Cu, 0.3 at% Mg, 0.2 at% Ag, 0.02 at% Zr, 0.7 at% Sc, the measured concentration of other elements is negligible, Li could not be detected) confirms the composition of main constituent elements within the experimental error of EDS measurements (compare with **Table 1**). A relatively low concentration of Zr in the vicinity of the boundary phase could reflect its inhomogeneous distribution imposed by the peritectic character of Al-Zr solidification at low Zr concentrations [19]. Therefore, a slightly higher Zr concentration could be expected inside the originally solidified grains than in their outer rim.

Detection of Li, unfeasible by STEM and EDS analyses, partially limits the current investigation because the absence or the existence of complex Li-containing primary phases in the as-cast alloy could not be confirmed. More detailed analyses using methods linked to TEM (selected area electron diffraction) or X-ray analysis could help to solve this problem. However, numerous experiments performed on conventionally cast Al-Li-based alloys show that the probability of forming Li-containing particles during solidification is very low for alloys containing Li below 1 wt% and almost zero for Li concentrations close to 0.5 wt% [20].

Figure 2 shows the same area imaged using SEM detectors in topographic and composition contrasts. Not surprisingly, only some surface undulations identifying only partially the particle morphology could be recognized in the topographic mode in both BSE and SE detectors. Much better correspondence with STEM HAADF and BF images could be found with both SEM detectors operated in composition contrast mode, proving thus that the majority of the particle should be situated in the volume of the foil or even pointing out of the lower surface of the foil - a fact, which could not be confirmed by STEM.

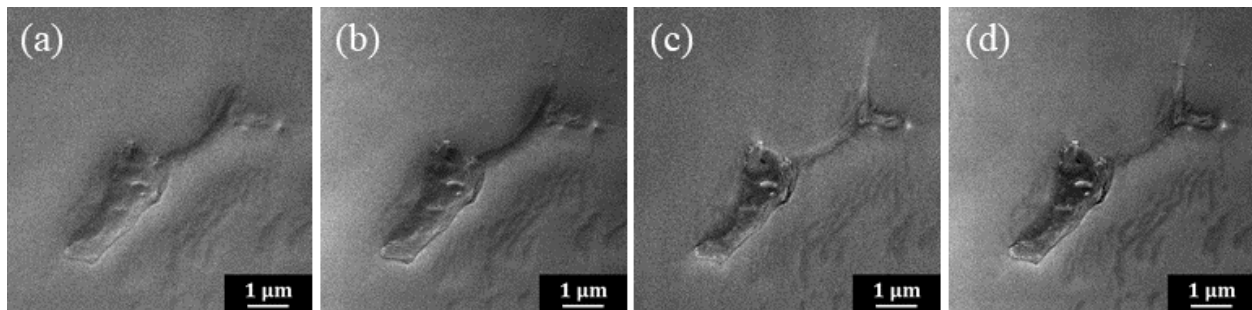


Figure 2 The same particle as in **Figure 1** is acquired in SEM BSE (a) and SE (b) topographic modes, and SEM BSE (c) and SE (d) composition contrasts.

Similar STEM/SEM/EDS analyses were performed on a series of grain-boundary particles in the as-cast state. Generally, the structural features of all analyzed particles are almost the same. They always contain Al, Cu, Fe, and a minor fraction of Mg. None of them contains Zr, Sc, or Ag, confirming thus that Zr, Sc, and Ag are dissolved in the matrix. For example, **Figure 3** shows the STEM/EDS analysis of another grain boundary particle. This particle contains (point 1 in **Figure 3a**) Al, Cu, Mg, and Fe as main constituent elements with concentrations corresponding with the previous particle (62 at% Al, 6 at% Fe, 31 at% Cu, 1 at% Mg), and similar composition of the surrounding matrix (point 2 in **Figure 3** - 96 at% Al, 3 at% Cu, 0.2 at% Mg, 0.1 at% Ag, <0.03 at% Zr, 0.4 at% Sc).

Transformation of primary phase particles during the in-situ annealing is documented on the particle analyzed in **Figures 1 and 2** (**Figure 4**). The first significant changes in the morphology could be detected at 450 °C. Cu-rich parts (marked by arrows) dissolve at this temperature. Only subtle modifications and spheroidisation of particles in the Fe-containing parts proceed with increasing temperature, in accordance with similar observations of Liu et al. [17].

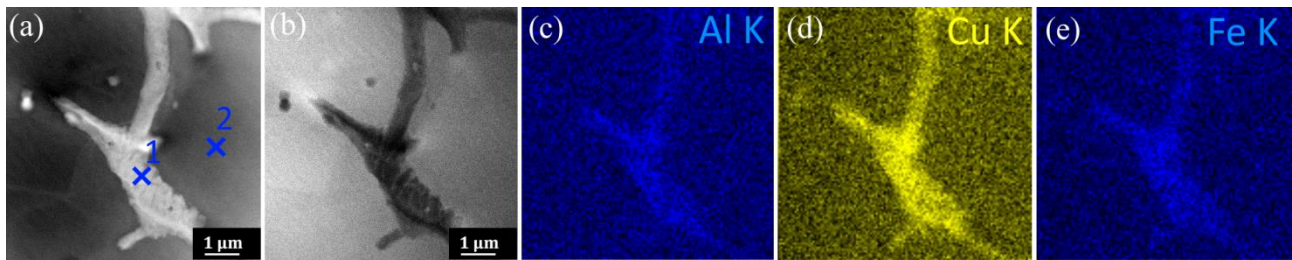


Figure 3 STEM HAADF (a), STEM BF (b), and distribution maps of Al (c), Cu (d), and Fe (e) in the primary phase particle

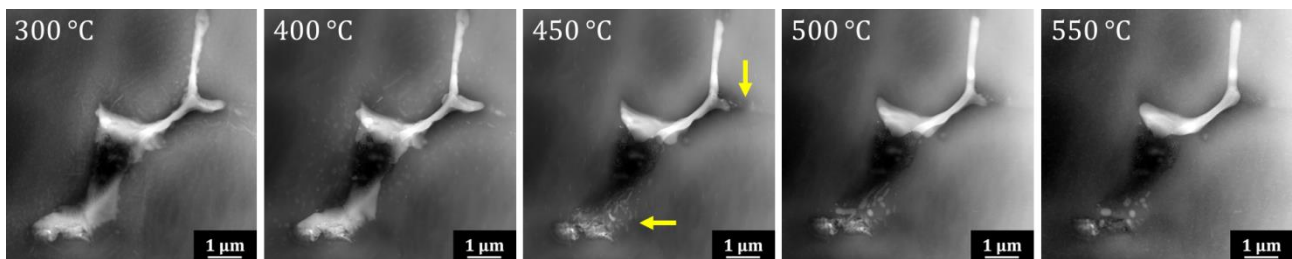


Figure 4 STEM HAADF images of the primary phase particle during in-situ annealing

Figure 5 shows the same area after step-by-step annealing up to 550 °C and a rapid (in-situ) cooling down of the specimen to room temperature. A significant part of the particle is partially dissolved or transformed into smaller particles. In contrast, the part of the original particle situated in the upper right corner is unaffected by the elevated temperature. This effect is probably caused by the fact that this part of the primary particle is not in direct contact with the Al matrix and points out of the bottom surface of the foil due to an inhomogeneous electrolytic etching. Another possible explanation is based on the value of the diffusion coefficient of Fe in intermetallic particles, which is significantly lower than the one in the aluminum matrix [21,22]. EDS maps show that Cu and Fe are both still present in newly formed particles and the untransformed part of the original one, indicating most probably the presence of the Al_7Cu_2Fe phase.

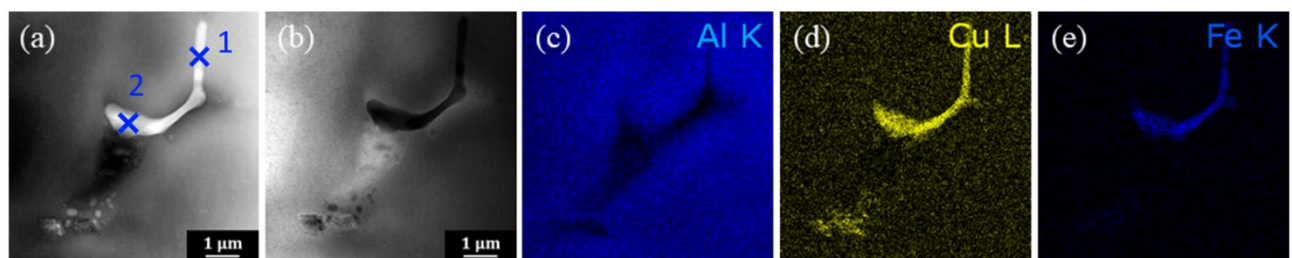


Figure 5 STEM HAADF (a), BF (b), and distribution maps of Al (c), Cu (d), and Fe (e) in the specimen annealed up to 550 °C, and in-situ cooled down to room temperature

4. CONCLUSIONS

Twin-roll cast Al-Li-Cu-Mg-Zr-Sc alloy was studied by in-situ STEM/SEM and EDS during heating up to 550 °C. The as-cast material contains Cu- or Cu+Fe-rich complex phases at grain boundaries. EDS analysis indicates the formation of AlCu (Al_2Cu) and Al_7Cu_2Fe phases during the TRC process. The presence of Li in complex boundary phases could not be excluded due to the limitations of EDS analysis. However, the participation of Li in their formation is relatively very low considering the low Li nominal concentration. The presence of Zr, Sc, or Ag in the grain boundary phases was not observed, indicating that these elements, similarly to Li, were fully dissolved in the solid solution and did not interact with grain boundary phases. Particles of the Cu-rich phase dissolve at 450 °C. A spheroidisation of smaller Al_7Cu_2Fe particles occurs at higher annealing temperatures.

In contrast, coarser Al₇Cu₂Fe particles remain unaffected by the annealing, most probably due to the low diffusion coefficient of Fe in the intermetallic compound.

ACKNOWLEDGEMENTS

The authors would like to thank the project of the Czech Science Foundation number 20-19170S and the German Research Foundation (Deutsche Forschungsgemeinschaft (DFG)) for financial support within the scope of project SCHA 1484/46-1.

REFERENCES

- [1] ZHAO, T.B., SATO, Y.S., XIAO, R.S., HUANG, T., ZHANG, J.Q. Hardness distribution and aging response associated with precipitation behavior in a laser pressure welded Al-Li alloy 2198. *Mater. Sci. Eng. A*. 2021, vol. 808, p. 140946.
- [2] CHEN, L., HU, Y.N., HE, E.G., WU, S.C., FU, Y.N. Microstructural and failure mechanism of laser welded 2A97 Al-Li alloys via synchrotron 3D tomography. *Int. J. Lightweight Materials and Manuf.* 2018, vol. 1, pp.169-178.
- [3] BALDUCCI, E., CESCHINI, L., MESSIERI, S., WENNER, S., HOLMESTAD, R. Effects of overaging on microstructure and tensile properties of the 2055 Al-Cu-Li-Ag alloy. *Mater. Sci. Eng. A*. 2017, vol. 707, pp. 221-231.
- [4] XIAO, R., ZHANG, X. Problems and issues in laser beam welding of aluminum-lithium alloys. *J. Manuf. Process.* 2014, vol. 16, pp. 166-175.
- [5] LAVERNIA, E.J., GRANT, N.J. Aluminium-lithium alloys. *J. Mater. Sci.* 1987, vol. 22, pp. 1521-1529.
- [6] KAYSHAP, B., CHATURVEDI, M., STAIN, M. M. Strain anisotropy in AA8090 Al-Li alloy during high temperature deformation. *Mater. Sci. Eng. A*. 2020, vol. 281, pp. 88-95.
- [7] QIN, H., ZHANG, H., WU, H. The evolution of precipitation and microstructure in friction stir welded 2195-T8 Al-Li alloy. *Mater. Sci. Eng. A*. 2015, vol. 625, pp. 322-329.
- [8] RIOJA, R, LIU, J. The evolution of Al-Li base products for aerospace and space applications. *Metall. Mater. Trans. A*. 2012, vol. 43, pp. 3325-3337.
- [9] DURSUN, T., SOUTIS, C. Recent developments in advanced aircraft aluminium alloys. *Mater. Des.* 2014, vol. 56, pp. 862-871.
- [10] KIM, I.S., SONG, M.Y., KIM, J.H., HONG, S.K. Effect of added Mg on the clustering and two-step aging behavior of Al-Cu alloys. *Mater. Sci. Eng. A*. 2020, vol. 798, p. 140123.
- [11] CHEN, H., CHEN, Z., JI, G., ZHONG, S., WANG, H., BORBELY, A., KE, Y., BRECHET, Y. Experimental and modelling assessment of ductility in a precipitation hardening AlMgScZr alloy. *Int. J. Plasticity*. 2021, vol. 139, p. 102971.
- [12] ZHANG, J., WU, G., ZHANG, L., ZHANG, X, SHI, C., TONG, X. Addressing the strength-ductility trade-off in a cast Al-Li-Cu alloy-Synergistic effect of Sc-alloying and optimized artificial ageing scheme. *J. Mater. Sci. Technol.* 2022, vol. 96, pp. 212-225.
- [13] SUN, Z., HE, B., CHEN, R., WANG, H. Anomalous precipitation of Al₃Sc dispersoids on deformation behavior of a novel Al-Cu-Li alloy fabricated by direct energy deposition. *Mater. Lett.* 2022, vol. 318, p. 132207.
- [14] KNIPLING, K.E., SEIDMAN, D.N., DUNAND, D.C. Ambient- and high-temperature mechanical properties of isochronally aged Al-0.06Sc, Al-0.06Zr and Al-0.06Sc-0.06Zr (at.%) alloys. *Acta Mater.* 2011, vol. 59, pp. 943-954.
- [15] LI, S., WEI, B., XU, J., XU, G., LI, Y., WANG, Z. High solid-solution strengthening mechanism of a novel aluminum-lithium alloy fabricated by electromagnetic near-net shape technology. *Mater. Sci. Eng. A*. 2022, vol. 829, p. 142148.
- [16] GRYDIN, O., STOLBCHENKO, M., SCHAPER, M., BELEJOVÁ, S., KRÁLÍK, R., BAJTOŠOVÁ, L., KŘIVSKÁ, B., HÁJEK, M., CIESLAR, M. New twin-roll cast Al-Li based alloys for high-strength applications. *Metals*. 2020, vol. 10, p. 987.

- [17] LIU, Q., ZHU, R.H., Li, J.F., CHEN, Y.L., ZHANG, X.H., ZHANG, L., ZHENG, Z.Q. Microstructural evolution of Mg, Ag and Zn micro-alloyed Al-Cu-Li alloy during homogenization. *Trans. Nonferrous Met. Soc. China*. 2016, vol. 26, pp. 607-619.
- [18] WANG, S.S., JIANG, J.T., FAN, G.H., PANINDRE, A.M., FRANKEL, G.S., ZHEN, L. Accelerated precipitation and growth of phases in an Al-Zn-Mg-Cu alloy processed by surface abrasion. *Acta Mater*. 2017, vol. 131, pp. 233-245.
- [19] JANGHORBAN, A., ANTONI-ZDZIOBEK, A., LOMELLO-TAFIN, M., ANTION, C., MAZINGUE, Th., PISCH, A. Phase equilibria in the aluminium-rich side of the Al-Zr system. *Journal of Thermal Analysis and Calorimetry*. 2013, vol. 114, pp. 1015-1020.
- [20] WU, L., LI, X., WANG H. The effect of major constituents on microstructure and mechanical properties of cast Al-Li-Cu-Zr alloy. *Mater. Char.* 2021, vol. 171, p. 110800.
- [21] EGGERSMANN, M., MEHRER, H. Diffusion in intermetallic phases of the Fe-Al system. *Philos. Mag. A*. 2000, vol. 80, pp. 1219-1244.
- [22] DU, Y., CHANG, Y.A., HUANG, B., GONG, W., JIN, Z., XU, H., YUAN, Z. LIU, Y., HE, Y., XIE, F.-Y. Diffusion coefficients of some solutes in fcc and liquid Al: Critical evaluation and correlation. *Mater. Sci. Eng. A*. 2003, vol. 363, pp. 140-151.